

Multiple Adsorption of NO on Fe²⁺ Cations in the α - and β -Positions of Ferrierite: An Experimental and Density Functional Study

L. Benco,^{*,†,‡} T. Bucko,[†] R. Grybos,[†] J. Hafner,[†] Z. Sobalik,[§] J. Dedecek,[§] S. Sklenak,[§] and J. Hrusak[§]

Fakultät für Physik and Center for Computational Materials Science, Universität Wien, Sensengasse 8, A-1090 Wien, Austria, Institute of Inorganic Chemistry, Slovak Academy of Sciences, Dubravska cesta 9, SK-84536 Bratislava, Slovak Republic, and J. Heyrovsky Institute of Physical Chemistry, Academy of Sciences of the Czech Republic, Dolejskova 3, CZ-18223 Prague 8, Czech Republic

Received: March 27, 2007; In Final Form: April 26, 2007

Adsorption of NO on Fe-exchanged ferrierite is investigated by Fourier transform infrared (FTIR) spectroscopy and ab initio periodic density functional theory (DFT) calculations. The adsorption properties of single Fe species located in the β - and α -site representing the two most stable locations of the extraframework cation are probed. We consider a divalent Fe(II) cation with two framework Al/Si substitutions, three configurations with two Al atoms in the six-membered ring separated by the $-\text{Si}-\text{O}-\text{Si}-$ chain, and one configuration with two Al atoms in different channels representing a low-Al zeolite. Upon adsorption of a single NO molecule, a tetragonal pyramid forms with four in-plane Fe–O bonds to the framework and one axial Fe–N bond. Upon adsorption of a second NO molecule on a Fe²⁺ cation in the β -2, α -1, and α -2 sites, a cis tetrahedral complex is formed. In the most stable configuration in the β -1 site, however, the planar Fe–O bonding is not destroyed but is completed to a trans octahedral complex. The tetrahedral complex contains an extraframework [Fe–(NO)₂]⁺ (dinitrosyl) particle, carrying only a single positive charge. Because such a particle compensates only one Al/Si substitution, the resulting charge imbalance induces a high chemical reactivity of the framework Al sites. A third NO molecule therefore adsorbs on the activated oxygen atoms next to the Al site whose charge remains unbalanced, and it is oxidized to NO⁺. NO stretching frequencies of adsorption clusters formed in Fe–FER are similar to those recorded on Fe–ZSM-5 and Fe–silicatite. The calculated NO stretching frequencies agree well with experimental data and support the proposed assignment to mono-, di-, and trinitrosyl species. Before a trinitrosyl species is formed, one NO molecule adsorbs on the Al site and converts to NO⁺. The calculated stretching frequencies of the NO⁺ cation agree with the IR band at 2000–2100 cm⁻¹.

1. Introduction

Fe-exchanged zeolites are efficient catalysts for N₂O decomposition.^{1–8} The mechanism proposed for the decomposition consists of a sequence of reaction steps involving N₂O, NO, NO₂, N₂, and O₂ molecules and an oxygen atom deposited on the active site.^{9,10} The complex system of individual reactions is associated with changes of the oxidation state of the extraframework cation and involves a promoting effect of NO on N₂O decomposition.⁹ Some experiments indicate a cooperation of two neighboring Fe sites,^{5,10–12} whereas others stress the isolated character of the active Fe species.¹³ In spite of numerous investigations of the relationship between the structure of Fe-exchanged zeolites and their performance in N₂O decomposition, the nature of active site and the mechanism of the conversion are not fully understood.

Several theoretical studies report simulated pathways for N₂O decomposition over an Fe-exchanged zeolite. Cluster calculations have been performed by Zhidomirov and co-workers,^{14–16} Yoshizawa and co-workers,^{17,18} and Bell and co-workers.^{19–21} Zhidomirov and co-workers consider both a bare Fe²⁺ cation

and various oxo-species of mono- and binuclear Fe complexes as intrazeolite active sites. An isolated Fe cation has been studied by Yoshizawa et al., while a large variety of surface hydroxo- and oxo-species is considered by Bell and co-workers. They reported a network of over 100 elementary reactions for the direct and NO-assisted decomposition of N₂O. All reactions are simulated on an iron cluster compensating one framework Al/Si substitution. In an active zeolite, most of the extraframework Fe species contain divalent Fe²⁺ cations. A monovalent particle compensating just one Al/Si substitution does not represent a good model of the active site because for such a configuration a change of the oxidation state of the transition-metal cation is strongly limited. In spite of the oversimplified model, good agreement with experimental results is reported. Recently, a periodic density functional theory (DFT) study of the decomposition of N₂O has been reported, with the Fe²⁺ cation in the α -position of ferrierite chosen as a model for the investigation of benzene-to-phenol oxidation.²²

Ferrierite is an industrial zeolite relevant for catalytic applications. The size of the unit cell, containing 108 atoms, allows ab initio treatment of the full periodic structure. In our recent work,²³ we investigated the adsorption of a single NO molecule in Fe-exchanged ferrierite. The calculated adsorption energies show two different classes of adsorption sites. A Fe²⁺ cation in a β -site forms a very stable configuration but leads to adsorption

* To whom correspondence should be addressed. E-mail: lubomir.benco@univie.ac.at.

[†] Universität Wien.

[‡] Slovak Academy of Sciences.

[§] Academy of Sciences of the Czech Republic.

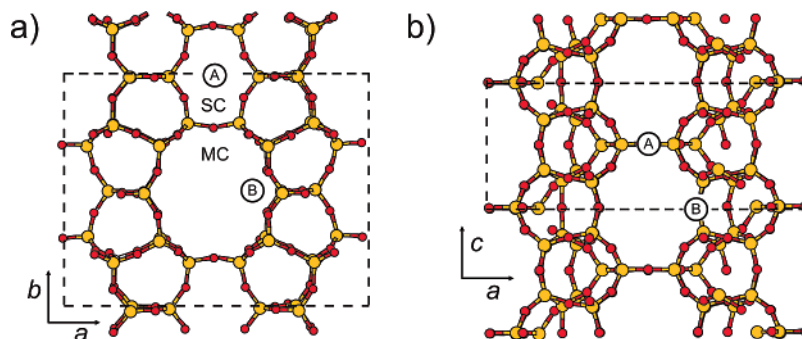


Figure 1. The ferrierite structure and the most frequent positions of extraframework cations. (a) Top view of the structure showing the main channel (MC) and the side channel (SC). Dashed lines represent the unit cell with *Immm* symmetry. (b) Side view along the **b** vector. The most populated positions of extraframework cations are marked by A (β -site) and B (α -site).

energies of only ~ 180 kJ/mol. In contrast, a less stable configuration with Fe^{2+} in the α -site exhibits a much higher adsorption energy of ~ 240 kJ/mol. The strong interaction between NO and the Fe^{2+} cation in both the α - and β -sites suggests, however, that the bonding capacity of the transition-metal cation is not exhausted with the adsorption of just one molecule. The increasing number of the NO stretching bands in the IR spectra of Fe-exchanged zeolites with increasing pressure of NO indicates bonding of several sorbate molecules to one cation. On the basis of the variation of band intensities, Berlier and co-workers suggested the existence of dinitrosyl and trinitrosyl adsorption species. According to their assignment for Fe-ZSM-5,²⁴ Fe-MCM-22,²⁵ and Fe-silicalite,²⁶ the bands at ~ 1770 cm^{-1} and ~ 1845 cm^{-1} correspond to the asymmetric and the symmetric component of the concerted stretching in dinitrosyl species and the bands at ~ 1920 cm^{-1} and ~ 1825 cm^{-1} are assigned to the NO stretching modes in trinitrosyl species.

In our present study, the adsorption properties of Fe^{2+} cations in extraframework positions of ferrierite are probed both experimentally and theoretically. IR spectra of Fe-exchanged ferrierite are recorded as a function of the pressure of NO and are compared with those reported for other zeolites. In addition, DFT calculations of NO adsorbed at extraframework Fe^{2+} cations, representing the most active site of the zeolite, have been performed for cation locations comparable with those determined by structural analysis. The number of adsorbed NO molecules is stepwise increased until all active sites of the zeolite are fully saturated. For each coverage, the activity of different sites, such as the Fe^{2+} cation, partially coordinated Fe^{2+} , and Al sites of the framework, is inspected. To validate the geometry of the intrazeolite cluster formed upon adsorption, calculated NO stretching frequencies are confronted with the measured IR stretching bands of ferrierite and are compared with IR spectra of other zeolites.

2. Experimental Section

NH_4 -FER (Si/Al 8.4) was prepared by ion-exchange with a 0.2 M NH_4OH solution at room temperature from materials supplied by TOSOH, Japan. The zeolite in the NH_4 form was granulated into 0.3–0.6 mm grains and was dried at 150 $^\circ\text{C}$ for 6 h. About 1 g of the zeolite grains was then wetted by about 1.5 mL of impregnation solution. The impregnation solution was prepared by dissolving 0.02–0.3 g FeCl_3 in 14 g of acetylacetone. The mixture was stirred and left at room temperature (RT) for 5 h. Then, the grains were separated and dried. The samples were evacuated for 1 h at 100 $^\circ\text{C}$, and then the temperature was increased to 350 $^\circ\text{C}$ and was kept at that temperature for 3 h. After cooling to room temperature, the

sample was washed in 800 mL of distilled water, was filtered, and was dried on air at RT.

IR spectra were recorded over the 4000–400 cm^{-1} region at room temperature using a Fourier transform infrared (FTIR) spectrometer Magna-550 (Nicolet) equipped with an MCT-B liquid-nitrogen-cooled detector, using a heatable cell with KBr windows and connected to a vacuum system and a glass ampule with d_3 -acetonitrile. Samples were measured in the form of self-supporting pellets (about 10 mg/cm^2). Usually, 200 scans were recorded at resolution of 2 cm^{-1} for a single spectrum. IR spectra were normalized to the weight of 10 mg/cm^2 .

3. Structure and Computational Details

The structure of ferrierite exhibits a one-dimensional pore system. Figure 1 shows top (a) and side views (b) of the structure. The main channel (MC) extends along the *c* lattice vector. It is circumscribed by 10-membered rings (10MR) while the side channel (SC) is circumscribed by 8MRs. Both the MC and the SC are cross-linked with the 8MR channels extending along the **b** lattice vector (Figure 1b). The unit cell (space group symmetry *Immm*) is indicated in Figure 1 by dashed lines. In a purely siliceous zeolite, the cell contains 108 atomic positions, 36 tetrahedral (T) Si sites, and 72 O sites. Experimental cell parameters of dehydrated K-exchanged ferrierite are **a** = 18.651, **b** = 14.173, and **c** = 7.404 Å .²⁸ In Figure 1, A and B indicate two stable locations of the extraframework cation according to the classification by Mortier.²⁷

Sites A and B are both located in six-membered rings (6MR) of the zeolite framework. The A site, denoted also as a β -site,²⁹ represents the most stable location of the extraframework cation.

In our recent study of stabilities and adsorption capacities of active sites in Fe-FER, we reported that the stability of a particular configuration depends critically on the location of the Al/Si substitutions.²³ For equivalent locations of Al atoms, the configuration with Fe^{2+} in the β -site is at least 30 kJ/mol more stable than that in the α -site.²³ This agrees with the experimental observation that the most frequent location of the extraframework cation is in the A (β)-site. The local configuration formed by anchoring the extraframework Fe^{2+} cation in the 6MR of the side channel (β -site) is displayed in Figure 2. A configuration with a cation in the 6MR of the main channel (α -site) is displayed in Figure 3.

To characterize the bonding of NO molecules to the Fe^{2+} cation and the interaction of sorbate molecules with the zeolite framework, DFT calculations using the Vienna ab initio Simulation Package (VASP)^{30–33} have been performed. The calculations are performed using the unit cell parameters of dehydrated ferrierite.²⁸ Multiple adsorption of NO is probed on the four stable local configurations of the extraframework Fe^{2+}

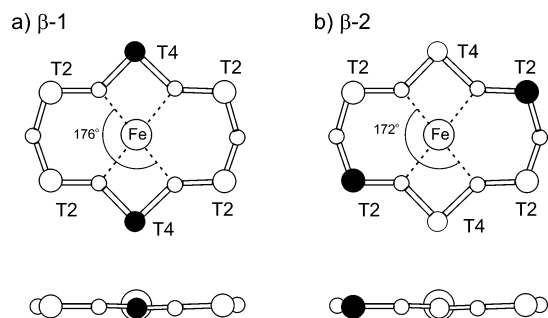


Figure 2. The local configuration with the Fe²⁺ cation in the β -site. Top/bottom panels show top/side views of the 6MR. (a) β -1 configuration with two Al/Si substitutions in T4-sites, (b) β -2 configuration with two T2-substitutions. Configuration β -2 is 116 kJ/mol less stable than β -1 (ref 23).

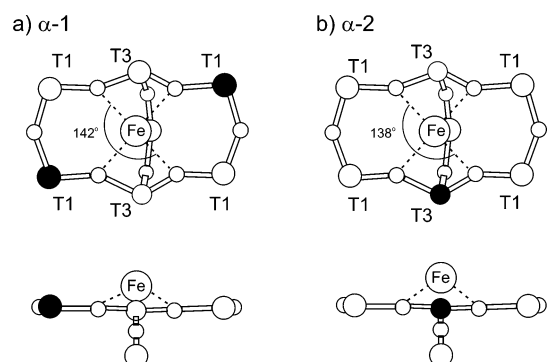


Figure 3. Local configuration with the Fe²⁺ cation in the α -site. Top/bottom panels show top/side views of the 6MR. (a) α -1 configuration with two Al/Si substitutions in T1-sites, (b) α -2 configuration with one T3-substitution and the second Al located in a T1 site of another 6MR. Configuration α -2 is 63 kJ/mol less stable than α -1 (ref 23).

cation displayed in Figures 2 and 3. The standard computational setup used for the relaxation of intrazeolite adsorption clusters is given in our previous work (PW91, $E_{\text{cutoff}} = 400$ eV).²³ Vibrational spectra have been calculated via ab initio molecular dynamics. The molecular dynamics simulations use the exact Hellmann–Feynman forces acting on atoms and apply the statistics of the canonical ensemble to the motion of the atomic nuclei³⁴ using the Verlet velocity algorithm.³⁵ The time step for the integration of the equations of motion is $\Delta t = 1$ fs. Stretching frequencies of adsorbed NO molecules are calculated via Fourier transform of the velocity autocorrelation function on the basis of a molecular dynamics (MD) simulation of 2 ps at 300 K. The MD simulations produce the temperature-dependent anharmonic frequencies. Harmonic stretching frequencies of NO molecules are calculated using the finite differences method.³⁶ The correction for anharmonicity is evaluated with the program Anharm.³⁷

4. Results and Discussion

The adsorption capacities and bonding properties of the extraframework Fe²⁺ cation are compared for two configurations with Fe²⁺ in the β -site (Figure 2) and two in α -sites (Figure 3). Three configurations contain a chain sequence –Al–Si–Si–Al–, which seems to be the most probable one in low-Al zeolites and energetically very favorable for divalent cations.³⁸ The configuration displayed in Figure 3b contains two Al/Si substitutions located in two different 6MRs connected via three T-sites occupied by Si (chain sequence –Al–Si–Si–Si–Al–). Not considered is the configuration with Fe²⁺ in the α -site and two Al/Si substitutions in T3 sites (Figure 3). The stability

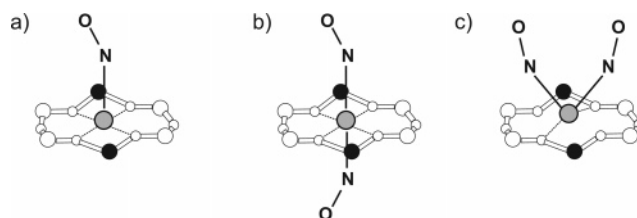


Figure 4. Configurations formed upon adsorption of NO on the β -1 site. (a) Mononitrosyl, (b) *trans*-dinitrosyl, and (c) *cis*-dinitrosyl. Full circles represent the Al atoms, a gray circle represents the Fe²⁺ cation, and small and large empty circles represent O and Si atoms.

of such a configuration is high and comparable with the most stable configuration formed in the β -site (Figure 2a). However, because of the chain sequence Al–Si–Al, the abundance of this configuration is extremely low, as indicated by NMR experiments.³⁸

4.1. Adsorption on Fe²⁺ in the β -Site. The extraframework Fe²⁺ cation anchored in the β -site forms the most stable Fe–FER configuration.²³ The oval shape of the 6MR allows two different locations of the Al–Si–Si–Al chain sequence, leading to the two configurations displayed in Figure 2. As reported in our recent work,²³ the configuration β -1 with Al in T4 sites (Figure 2a) is by 116 kJ/mol more stable than β -2 with Al in T2 sites (Figure 2b). In both configurations, Fe²⁺ forms four nearly coplanar Fe–O bonds with O–Fe–O angles of 176° (172°) and average Fe–O distances of 2.003 Å (2.041 Å). The higher stability of configuration β -1 results from the formation of four Fe–O bonds with oxygen atoms activated by a neighboring Al atom, while in β -2 only two of the bonds are with activated oxygen atoms.

4.1.1. β -1 Site. Configurations formed upon adsorption of NO on an Fe²⁺ cation on the β -1 site are displayed in Figure 4. Strong bonding of Fe²⁺ with four framework O atoms next to Al sites leads to a planar coordination of the transition-metal cation with the cation approximately in the center of the 6MR. Adsorption of one molecule leads to a configuration with NO in a tilted axial position (Figure 4a). Two NO molecules can be adsorbed either in axial *trans* positions (Figure 4b) or in *cis* positions (Figure 4c). Geometric parameters, adsorption energies, NO stretching frequencies, and magnetic moments of the Fe-exchanged zeolite and adsorption clusters are collected in Table 1. The adsorption energies of a single NO molecule on Fe–FER with different locations of the cation range between 175 kJ/mol and ~260 kJ/mol.²³ With decreasing stability of the configuration, the adsorption energy of NO increases. The Fe²⁺ cation in the β -1 site forms the most stable configuration and therefore exhibits the lowest adsorption energy of 175 kJ/mol. Adsorption of NO induces a slight shortening of the Al–O distances in the surrounding zeolite framework. The Fe–O distances increase from 2.003 Å to 2.070 Å, and the O–Fe–O angles decrease from 176° to 145°. This shows that the adsorption of a NO molecule pulls the Fe²⁺ cation out of the plane of the 6MR.

Upon adsorption of a second molecule in a *trans* position, the quasi planar configuration is restored with O–Fe–O angles close to 180° (cf. Figure 4b). Two NO molecules in axial positions complete a quasi octahedral coordination of the transition-metal cation. The adsorption energy of the second molecule is only 58 kJ/mol. The elongation of both the Fe–N and the N–O distances indicates a considerable weakening of the bonding within the ON–Fe²⁺–NO cluster. The bond length of a single NO molecule adsorbed on the Fe²⁺ cation is 1.165 Å, and the NO stretching frequency corrected for anharmonicity is 1881 cm⁻¹. This value is in good agreement with the

TABLE 1: Geometric Parameters, Adsorption Energies, NO Stretching Frequencies, and Magnetic Moments of Fe-(NO)_x (x = 1, 2) Clusters Formed in the β-1 Site^a

configuration	Fe-FER	NO-Fe-FER	<i>trans</i> -(NO) ₂ -Fe-FER	<i>cis</i> -(NO) ₂ -Fe-FER
<i>r</i> _{Al-O} (av)	1.813	1.810	1.805	1.798
<i>r</i> _{Fe-O} (av)	2.003	2.070	2.003	2.178
O-Fe-O (av)	176	145	179	129
<i>r</i> _{Fe-N}		1.722	1.828, 1.818	1.736, 1.992
<i>r</i> _{N-O}		1.165	1.171, 1.173	1.161, 1.161
Fe-N-O		169	130, 131	129, 174
O-N-N-O			68	305
<i>E</i> _{ads} (NO)		175	233 (175 + 58)	205 (175 + 30)
<i>f</i> _{NO}		1881	1798, 1691	1889, 1795
magnetic moment	4	3	0	2

^a Energies in kJ/mol, distances in Å, angles in degrees, stretching frequencies in cm⁻¹, and magnetic moments in μ_B.

experimental stretching frequency of 1876 cm⁻¹ reported below for an Fe-FER as well as with NO in Fe-ZSM-5.²⁴ The bond weakening induced by the adsorption of the second NO molecule leads to an elongation of the NO bond length to 1.171 and 1.173 Å, respectively. The calculated stretching frequencies are 1798 and 1691 cm⁻¹. Interestingly, the asymmetrical and the symmetrical components of the stretching mode are both shifted to lower frequencies compared with the frequency of a single adsorbed NO molecule of 1881 cm⁻¹. The adsorbed NO molecules are tilted with respect to the orientation of the Fe-N bond. With an Fe-N-O angle of ~169°, the tilting is modest for the single molecule, and it is much stronger after adsorption of the second molecule (Fe-N-O ~ 130°). The O-N-N-O dihedral angle is 68°. Both the bare Fe²⁺ cation and Fe²⁺-NO cluster prefer high-spin configurations with magnetic moment of 4μ_B and 3μ_B, respectively. The extraframework Fe²⁺-(NO)₂ cluster, on the other hand, is nonmagnetic.

In the *cis* cluster (Figure 4c), the average Fe-O distance increases to 2.178 Å, and the average O-Fe-O angle decreases to 129°. In contrast to a planar bonding with four O atoms in the octahedron (Figure 4b), in the *cis* coordination displayed in Figure 4c, the transition-metal atom is pulled out of the plane of the 6MR and the two framework oxygens and the two N atoms of the adsorbed molecules form a tetrahedron around the cation. The distortion of the planar bonding leads to differences in the Fe-N distances and the Fe-N-O angles of the two adsorbed molecules. Surprisingly, in the *cis* cluster, both NO molecules have the same bond length of 1.161 Å. The energy of the distorted *cis* cluster is higher by 28 kJ/mol compared with the *trans* cluster.

Of the eight O atoms activated by two Al/Si substitutions, four atoms in the plane of the 6MR form Fe-O bonds (Figures 2a and 4). The other four O atoms are located such in the framework that they cannot interact with the extraframework cation or with sorbent molecules (see Figure 1). The Fe²⁺-(NO)₂ cluster anchored in the β-1 site thus represents a compact, relatively symmetrical and electronically well-balanced configuration. Strong Fe-O bonds fix the Fe²⁺ cation in the β-site and prevent displacements of the cation. The absence of

nonsaturated active sites makes the Fe²⁺-(NO)₂ cluster inert against interactions with other sorbate molecules.

4.1.2. β-2 Site. Configurations formed upon adsorption of one or two NO molecules at an Fe²⁺ cation in the β-2 site are displayed in Figure 5. Geometric parameters, adsorption energies, NO stretching frequencies, and magnetic moments are collected in Table 2. The adsorption geometries are similar to those formed on the β-1 site (cf. Figure 4). Adsorption of a single NO molecule leads to the same O-Fe-O angle of 145° for both the β-1 and β-2 sites. The change of bonding induced by *cis* adsorption of two molecules produces a distorted tetrahedral coordination of the cation, similar to that of the *cis* cluster on the β-1 site. In the β-2 site, the location of two Al atoms in T2-sites allows a strong local deformation of the framework. The change of coordination and the deformation of the 6MR are sketched in Figure 6. In the tetrahedral coordination, both the Fe-O and the Fe-N distances are considerably shortened compared with the octahedral coordination in the *trans* cluster. The transition from octahedral (*trans*) to tetrahedral (*cis*) coordination leads to more symmetric Fe-NO distances and angles (Table 2). The increase of the adsorption energy from 222 kJ/mol to 297 kJ/mol indicates the stability of the tetrahedral *cis* complex.

4.1.3. Stability of Mono- and Dinitrosyls on β-1 and β-2 Sites. The stabilities of mononitrosyl and dinitrosyl clusters formed by an Fe²⁺ cation in the β-1 and β-2 sites are compared in Table 3. A bare Fe²⁺ cation forms planar configurations with the Fe²⁺ cation in the center of the 6MR and four Fe-O bonds. In the β-2 site, however, only two bonds link to an activated O atom next to an Al site. The location of the Fe²⁺ cation in the β-2 site is therefore 116 kJ/mol less stable than that in the β-1 site. On both the β-1 and β-2 sites, the adsorption energy of the single NO molecule is 175 kJ/mol (Tables 1 and 2). Dinitrosyl complexes form either an octahedral *trans* cluster or a tetrahedral *cis* cluster. The most stable configuration is the *trans* cluster in the β-1 site which is lower in energy by 28 kJ/mol compared with the *cis* cluster. On the other hand, the *trans* cluster in the β-2 site is the least stable dinitrosyl complex. The adsorption of the second molecule in a *trans* position increases the energy difference relative to the β-1 site to 128 kJ/mol. The formation of a *cis* cluster in the β-2 site, on the other hand, is strongly stabilizing and decreases the energy difference between β-1 and β-2 from 116 kJ/mol to 52 kJ/mol.

4.1.4. Multiple NO Adsorption on the β-2 Site. The *trans* cluster anchored in the β-1 site represents a compact, relatively symmetrical, and electronically well-balanced configuration with completely filled bonding electronic levels and the Fermi level located at the upper edge of the main bonding band. The strong bonding of the Fe²⁺ cation to the framework prevents any

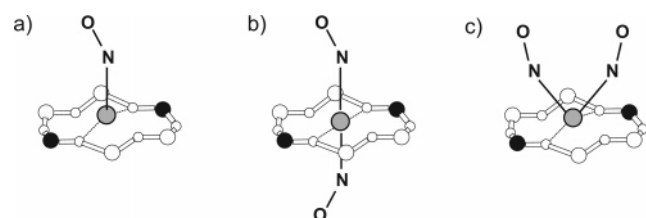


Figure 5. Configurations formed upon adsorption of NO on the Fe²⁺ cation in a β-2 site. (a) Mononitrosyl, (b) *trans*-dinitrosyl, and (c) *cis*-dinitrosyl.

TABLE 2: Geometric Parameters, Adsorption Energies, NO Stretching Frequencies, and Magnetic Moments of Adsorption Clusters Formed in the β -2 Site^a

configuration	Fe-FER	NO-Fe-FER	<i>trans</i> -(NO) ₂ -Fe-FER	<i>cis</i> -(NO) ₂ -Fe-FER
$r_{\text{Fe-O}}$ (av)	2.041	2.091	2.022	1.910
O-Fe-O (av)	172	145	171	134
$r_{\text{Fe-N}}$		1.724	1.964, 1.724	1.680, 1.682
$r_{\text{N-O}}$		1.164	1.169, 1.175	1.164, 1.164
Fe-N-O		167	147, 110	152, 152
O-N-N-O			185	358
$E_{\text{ads}}(\text{NO})$		175	222 (175 + 47)	297 (175 + 122)
$\tilde{\nu}_{\text{NO}}$		1883	1815, 1716	1887, 1824
magnetic moment	4	3	0	0

^a Energies in kJ/mol, distances in Å, angles in degrees, stretching frequencies in cm⁻¹, and magnetic moments in μ_{B} .

TABLE 3: Relative Energies of Fe²⁺-(NO)_x, x = 1, 2, Adsorption Clusters Formed in the β -1 and the β -2 Sites (kJ/mol)^a

configuration/site	β -1	β -2
Fe-FER	0	+116
NO-Fe-FER	0	+116
<i>trans</i> -(NO) ₂ -Fe-FER	0	+128
<i>cis</i> -(NO) ₂ -Fe-FER	+28	+52

^a The reference energy is the most stable configuration.

displacement of the transition-metal cation that could possibly lead to a configuration with increased adsorption capacity. The Fe²⁺ cation in the β -1 site is therefore completely saturated by two adsorbed NO molecules and is inert against further adsorption.

In contrast to the trans cluster for the tetrahedral cis cluster, the Fermi level lies deep in the bonding band. Unoccupied states above the Fermi level are able to accommodate electron density delivered by another adsorbed molecule. This indicates that the adsorption capacity of the cis cluster, formed in the β -2 site, is still not saturated and the cluster can adsorb further NO molecules. Figure 7 shows the differential adsorption energies for (NO)_x adsorption in ferrierite with the Fe²⁺ cation exchanged into the β -2 site for x = 1–4 (cf. Figure 2b). Adsorption on both the Fe²⁺ cation and the Al site is considered. We calculated the geometries of the adsorption clusters, the adsorption energies, the calculated adsorption energy is only 15 kJ/mol on the Al site (Figure 7b, left) and 175 kJ/mol on the Fe²⁺ cation (Figure 7b, right). The large difference indicates that at low pressures NO adsorbs exclusively on the Fe²⁺ cation. A second NO molecule also adsorbs on the transition-metal cation. The change of coordination from planar to tetrahedral results in a relatively high adsorption energy of the second molecule of 122 kJ/mol (Figure 7c, center). Formation of an octahedral trans cluster (Figure 7c, right) results in a low adsorption energy of 47 kJ/

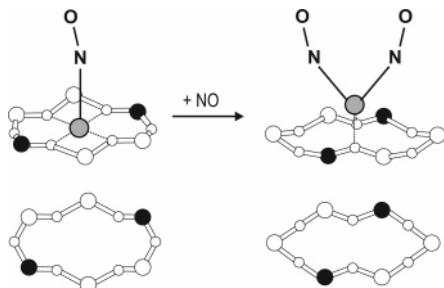


Figure 6. The change of bonding of Fe²⁺ in the β -2 site induced by adsorption of a second NO molecule. The coordination of the Fe²⁺ cation (top) and the top view of the 6MR (bottom) show the local deformation of the framework.

mol. Similarly, the Al site (Figure 7c, left) exhibits a low adsorption energy of only 34 kJ/mol. A third molecule binds to the Al site because direct bonding to the Fe²⁺ cation is less attractive. The differential adsorption energy on the Al site is 92 kJ/mol (Figure 7d, center). Because of the symmetrical configuration of the doubly coordinated Fe²⁺ cation in the β -2 site (cf. Figure 5c), adsorption on any of two Al sites leads to similar adsorption geometries and energies. Adsorption of a third molecule directly on the Fe²⁺-(NO)₂ cluster (Figure 7d, left) provides an adsorption energy of only 43 kJ/mol. In the presence of an octahedral trans cluster Fe-(NO)₂ (Figure 7d, right), the Al site exhibits no tendency to bind the third NO molecule. The calculated adsorption energy of 15 kJ/mol is as low as that calculated for the purely siliceous framework.

The adsorption of the third molecule on the Al site increases the adsorption capacity of the Fe-(NO)₂ cluster. Before the filling of the Al site, the adsorption energy of NO on Fe-(NO)₂ is 43 kJ/mol (Figure 7d, left). After the Al site is filled, the differential adsorption energy increases to 117 kJ/mol (Figure 7e, right). In a configuration with a *cis*-Fe-(NO)₂ cluster, the two Al sites (Figure 5c) are equally active. Figure 7e, left, shows that after one Al site is occupied the adsorption of NO on the second Al site provides a differential adsorption energy of only 38 kJ/mol. The integral adsorption energy for four NO molecules, three binding to the Fe²⁺ cation and one to an Al site, is 506 kJ/mol.

4.2. Adsorption on Fe²⁺ in the α -Site. The α -site is located in the center of a 6MR forming the side wall of the main channel, next to two T3 sites cross-linked by an O-Si-O chain (Figure 3). A cation exchanged into the α -site is located above the plane of the 6MR. The configuration with the cation at one side of the 6MR and the O-Si-O chain on the other side of the 6MR allows only *cis* configurations for multiple NO adsorption on the extraframework cation.

The differential adsorption energies for (NO)_x, x = 1–4, on the Fe²⁺ cation exchanged into the α -1 or α -2 site in ferrierite (Figure 3) are displayed in Figures 8 and 9, respectively. Decreasing stability of the configuration leads to an increase of the adsorption energy. The α -1 configuration is 35 kJ/mol less stable than β -2,²³ and the adsorption energy of a single NO molecule increases from 175 kJ/mol to 220 kJ/mol. Configurations α -1 and α -2 exhibit similar stabilities.²³ The adsorption energy of NO on Fe²⁺ in an α -2 site is even higher, 245 kJ/mol, because a transition-metal cation with only one Al site in its vicinity exhibits a higher bonding capacity. The schemes for successive NO adsorption in α -1 and α -2 sites (Figures 8 and 9) follow the same scenario as for the β -2 site (Figure 7). The first two molecules adsorb preferentially on the Fe²⁺ cation. A third molecule binds to an Al site. A fourth NO molecule adsorbs again on the transition-metal cation. A fifth

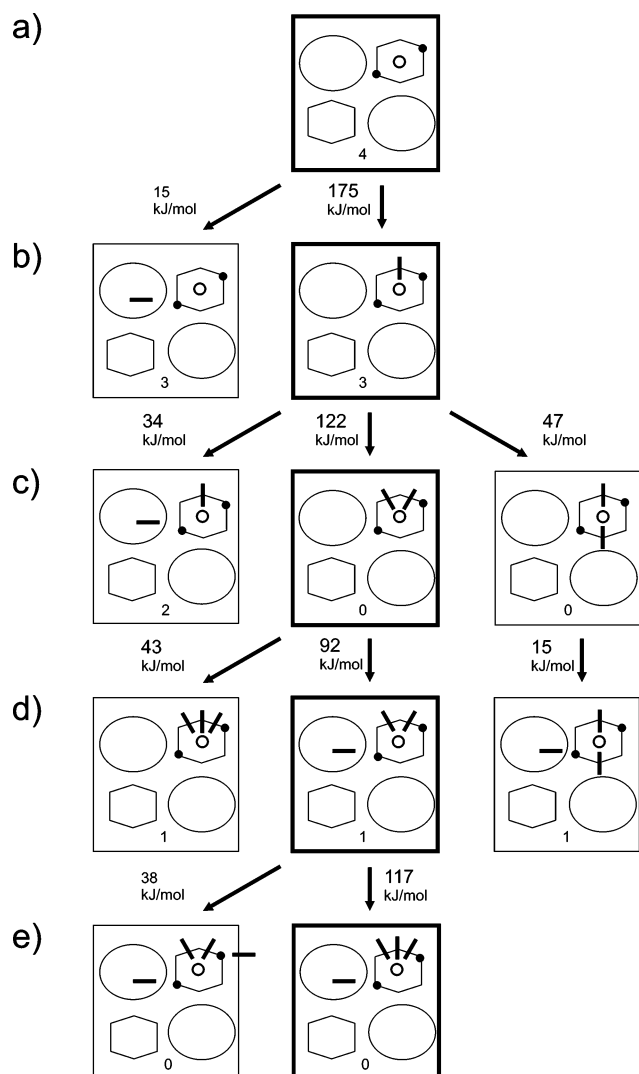


Figure 7. Differential adsorption energies of up to four NO molecules on Fe-FER with Fe²⁺ in the β -2 site. Ovals/hexagons represent main/side channels of the framework. Full/empty circles stand for Al/Fe atoms. Sticks indicate NO molecules. (a) Sorbent-free configuration, (b) mono-, (c) bi-, (d) tri-, and (e) tetra-adsorption. The arrow indicates the addition of one NO molecule. The differential adsorption energy in kJ/mol (next to the arrow) and the magnetic moment in μ_B (bottom of the panel) are listed for each configuration.

molecule is weakly adsorbed only in configuration α -2. The adsorption capacity of Fe²⁺ is completely saturated by three NO molecules (Figures 7–9, e). For the α -2 configuration exhibiting highest adsorption energies, the adsorption of a fifth NO molecule is still weakly exothermic. The highest adsorption energy is found for two NO molecules bound to the Al site located at a large distance from the Fe²⁺ cation (Figure 9f, left). The low value of ~ 40 kJ/mol, however, is comparable to adsorption in the siliceous framework. The cis cluster of the Fe²⁺ cation, formed in the β -2, α -1, and α -2 sites, is completely saturated with three NO molecules bound to the transition-metal cation and one NO molecule linked to an Al site. The integral adsorption energy of four NO molecules calculated for the α -1 and α -2 sites are 585 kJ/mol and 675 kJ/mol, respectively.

4.3. Properties of Adsorption Clusters. Adsorption clusters formed on the Fe²⁺ cation in different locations show similarities in bonding, magnetic properties, and NO stretching frequencies.

4.3.1. Adsorption on the Al Site. The differential adsorption energies displayed in Figures 7–9 show the importance of the interaction of a sorbate molecule with an Al site. Figure 10

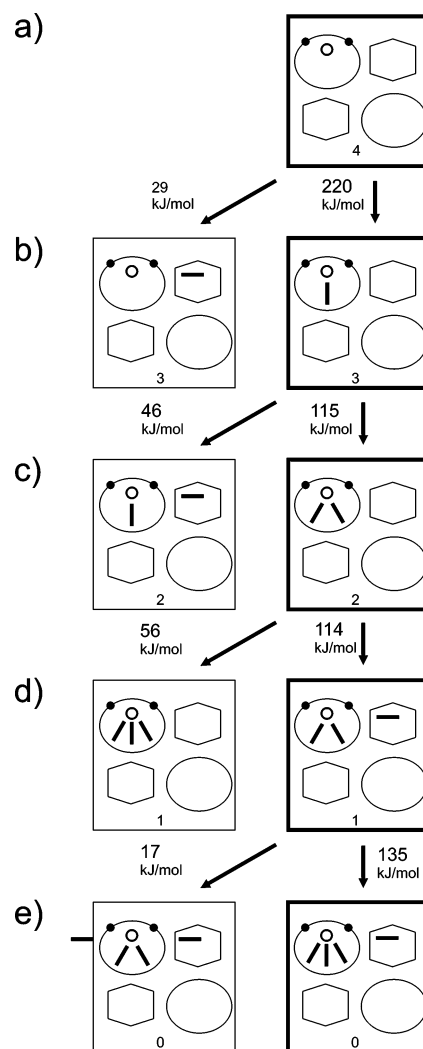


Figure 8. Differential adsorption energies of up to four NO molecules on Fe-FER with Fe²⁺ in the α -1 site. (a) Sorbent-free configuration, (b) mono-, (c) bi-, (d) tri-, and (e) tetra-adsorption. The differential adsorption energy of the configuration in kJ/mol (next to the arrow) and the magnetic moment in μ_B (bottom of the panel) are listed.

shows schematically the binding of a NO molecule to Al sites in configurations with the transition-metal cation located in β -1, β -2, α -1, or α -2 sites. The O atoms next to an Al site of the β -1 configuration (T4), located in the 6MR, all bind to the Fe²⁺ cation. Other activated O atoms are oriented into the framework and are not accessible from channels or cages of the zeolite. None of the Al sites of the β -1 configuration are thus accessible for the adsorption of sorbate molecules. The β -1 configuration therefore cannot adsorb more than two NO molecules, which bind in trans axial positions and form a stable distorted octahedral coordination shell around the Fe²⁺ cation. The Al sites of the β -2 configuration are located in the 8MR separating the side channel and the main channel. The adsorption cluster formed on the Fe²⁺ cation is located in the side channel. Both Al sites are thus exposed to interactions from the main channel. In Figure 10, a possible binding at the Al sites is indicated by arrows. The Al sites in the α -1 configuration are also accessible to adsorbed molecules (Figure 10c). The T1-sites in the main channel are accessible from cages above or below the 6MR of the side channel, as indicated by the arrows. In the configuration α -2, the Fe²⁺ cation binds to two O atoms next to an isolated Al site. This site is completely covered with the adsorption complex, but the second Al site is exposed to interactions with sorbate molecules (Figure 10d).

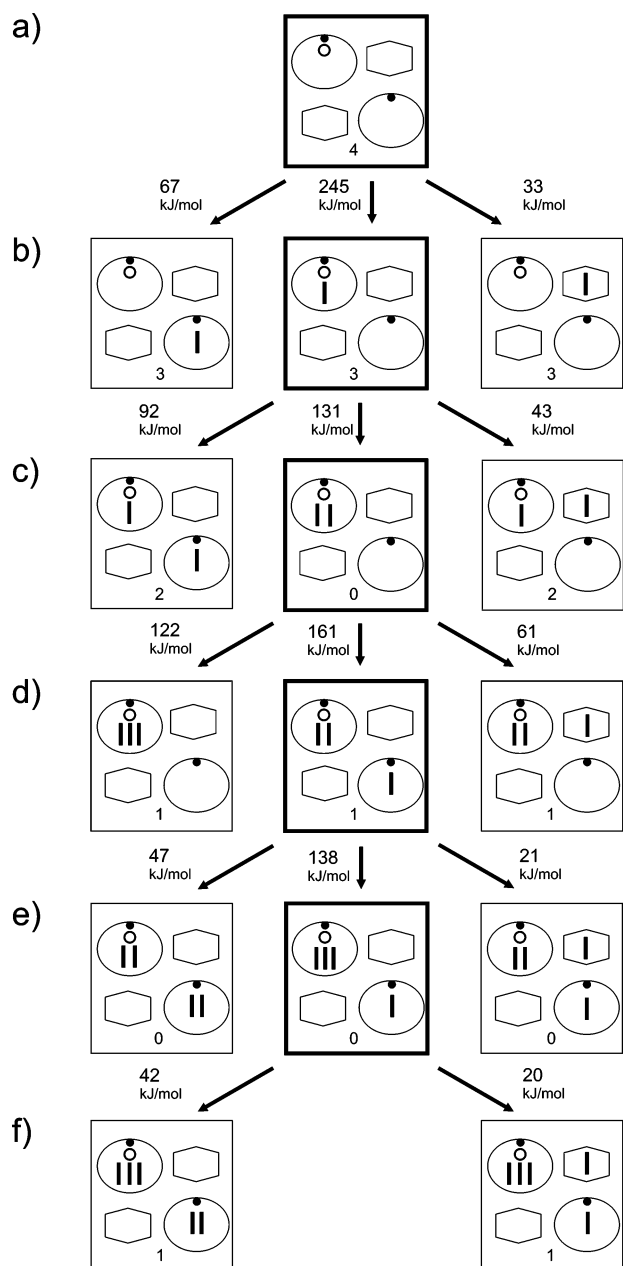


Figure 9. Differential adsorption energies of up to five NO molecules on Fe-FER with Fe²⁺ in the α -2 site. All symbols as in Figure 6. (a) Sorbent-free configuration, (b) mono-, (c) bi-, (d) tri-, (e) tetra-, and (f) penta-adsorption. The differential adsorption energy of the configuration in kJ/mol (next to the arrow) and the magnetic moment in μ_B (bottom of the panel) are listed for all adsorption complexes.

The bonding configuration of a NO molecule on an Al site is displayed in Figure 11. The molecule is located in an extraframework position next to the AlO₄ tetrahedron in the framework, similar to the position of an extraframework cation. The N atom binds to two activated framework O atoms at a distance of 2.13 Å and 2.37 Å, respectively. Relative to the Al-site, the adsorbed molecule is tilted exhibiting an Al...N–O angle of $\sim 130^\circ$. Both the tilted orientation of NO and the connection to two framework O atoms indicate bonding through N π -orbitals. Bond lengths of all adsorbed molecules differ from the bond length of 1.169 Å calculated for the free molecule. On the Al site, the NO molecule is shortened to 1.123 Å indicating a depletion of the antibonding $2\pi^*$ orbitals. In contrast, two NO molecules in the Fe–(NO)₂ cluster are elongated to 1.174 and 1.180 Å.

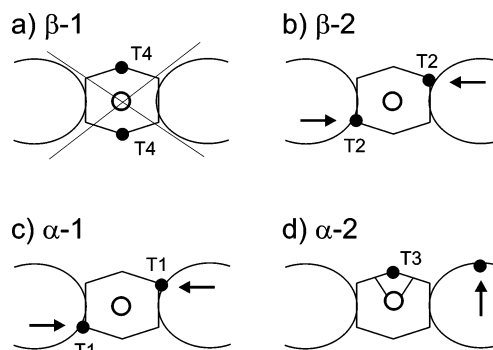


Figure 10. Schematic display of possible adsorption configurations of NO molecules on Al-sites in Fe-exchanged ferrierite. The arrows show binding configurations with the Fe²⁺ cation in the β -2, α -1, and α -2 sites.

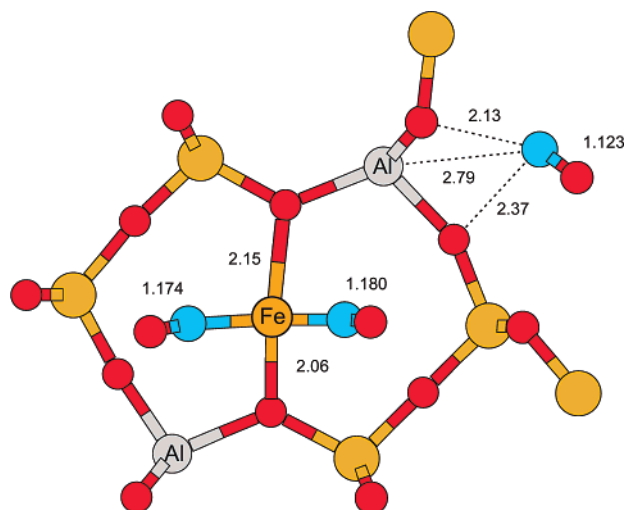


Figure 11. Bonding of NO to an Al site. The cis Fe–(NO)₂ cluster is located in the β -2 site and a third NO molecule binds to the Al site in the main channel (cf. Figure 10b). Light and dark gray circles in the framework represent Si and O atoms, respectively.

4.3.2. Changes of Bonding. During the stepwise adsorption of up to four NO molecules, extensive changes in the bonding of the transition-metal cation are observed. The geometrical changes are schematically displayed in Figure 12. The bare cation creates four bonds to O atoms of the framework, forming a nearly planar coordination of the transition-metal cation. Adsorption of one molecule leads to the formation of a FeO₄N complex forming a square pyramid (Figure 12b). The planar configuration is only weakly perturbed such that the Fe²⁺ cation is slightly displaced away from the zeolite framework. A pronounced change of bonding occurs upon adsorption of a second molecule. Two NO molecules bind directly to the Fe²⁺ cation and pull it away from the framework. The bonds with two adsorbed molecules and the remaining two bonds to framework O atoms form a distorted tetrahedral cluster (Figure 12c). This occurs upon adsorption of a second molecule on the Fe²⁺ cation in the β -2, α -1, and α -2 sites (step c in Figures 7–9). In the β -1 site, the second molecule prefers bonding in a trans position, forming an octahedral complex (Figure 4b). The tetrahedral *cis*-Fe–(NO)₂ cluster in β -2, α -1, and α -2 sites shows a large affinity of the Al site to adsorb the third NO molecule. Adsorption energies of NO on two O atoms next to the Al atom in the β -2, α -1, and α -2 configuration are 92, 109, and 161 kJ/mol, respectively. The adsorption of the third NO molecule on the Al site does not significantly change the bonding (Figure 12d). It induces, however, a shift of the Fe–

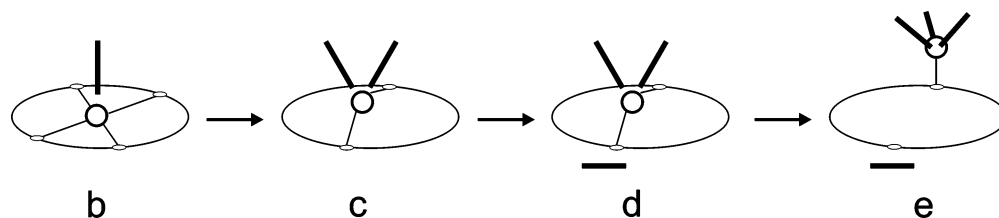


Figure 12. Schematic illustration of the change of bonding of a Fe^{2+} cation located in the β -2, α -1, and α -2 sites induced by the consecutive adsorption of up to four NO molecules. The planar FeO_4 coordination changes to tetrahedral $\text{O}_2\text{-Fe-N}_2$ and O-Fe-N_3 coordination. Letters (b–e) indicate adsorption steps in Figures 7–9.

(NO)₂ cluster toward the Al site not connected to the NO molecule. For the β -2 site, Figure 11 illustrates the asymmetry in the location of the $\text{Fe}-(\text{NO})_2$ cluster in the 6MR with Fe-O distances 2.05 and 2.16 Å, respectively. The fourth NO molecule binds to Fe and converts its coordination sphere from $\text{O}_2\text{-Fe-N}_2$ to O-Fe-N_3 with just one Fe-O bond to a framework O atom (Figure 12e). The tetrahedron is distorted toward the Al site without an adsorbed NO molecule. The separation of the NO molecule adsorbed close to the Al site and the $\text{Fe}-(\text{NO})_3$ cluster, and their location next to the Al sites indicates that both particles carry a single positive charge. The pronounced shortening of the NO bond length to 1.123 Å (Figure 11) is another piece of evidence that the NO molecule is electron depleted and is converted to a NO^+ cation. Multiple adsorption of NO on Fe-exchanged zeolite thus produces a configuration with a long-lived NO^+ cation bound to the inner surface of the zeolite.

4.3.3. Magnetic Properties. Bonding of the Fe^{2+} cation to a zeolite matrix conserves the high-spin configuration $\text{Fe } d^5 \uparrow d^1 \downarrow$ with a magnetic moment of $4\mu_B$ suggested by Hund's rule for the free Fe^{2+} cation. Adsorption of NO leads to the pairing of the $\text{NO } \pi^* \downarrow$ electron with an unpaired Fe d electron and to a decrease of the magnetic moment to $3\mu_B$ for the $\text{Fe}^{2+}\text{-NO}$ cluster in all intrazeolite configurations.²³ Adsorption of two NO molecules can lead to high- or low-spin states. On the β -1 and the β -2 sites, the octahedral *trans*- $\text{Fe}-(\text{NO})_2$ cluster is nonmagnetic, resulting from $\text{Fe } d_{12g}^6$, $\text{NO } \pi^* \uparrow$, $\text{NO } \pi^* \downarrow$ configuration. In tetrahedral *cis*- $\text{Fe}-(\text{NO})_2$ clusters, a distorted tetrahedral coordination conserves the low-spin configuration $\text{Fe } d_{eg}^4 d_{12g}^2 \uparrow$, and the pairing with two $\text{NO } \pi^* \downarrow$ electrons produces a nonmagnetic configuration. On the β -1 and α -1 site, the bonding is distorted toward a trigonal pyramid, and the *cis*- $\text{Fe}-(\text{NO})_2$ cluster carries a magnetic moment of $2\mu_B$. The bonding of one NO to the transition metal and of the second NO on another active site also leads to a high-spin state with a magnetic moment of $2\mu_B$. The adsorption of three and four NO molecules produces adsorption clusters with magnetic moments of $1\mu_B$ and $0\mu_B$, respectively.

4.3.4. NO Stretching Frequencies. FTIR spectra of Fe-FER with different Fe/Al ratios, measured after adsorption of NO at 25 Torr, are displayed in Figure 13. The dominant band is centered at 1876 cm^{-1} . The band is attributed to a mononitrosyl species on the Fe^{2+} cation. In our recent paper devoted to the DFT description of a NO adsorption on a Fe^{2+} cation at different locations in ferrierite,²³ we calculated NO stretching frequencies in good agreement with the experimental IR band at 1876 cm^{-1} . The position of the dominant band coincides with that measured on Fe-exchanged ZSM-5.²⁴ This indicates that the NO stretching frequency in the extraframework Fe-NO cluster is independent of the zeolite framework. In ferrierite with a high Fe/Al ratio, a multiplet of bands with two prominent peaks at 1824 and 1803 cm^{-1} is observed and much less intense, but clearly distinguished bands at ~ 1925 and ~ 1770 cm^{-1} are also observed. Similar modes are recorded on Fe-ZSM-5.²⁴ The pair of bands

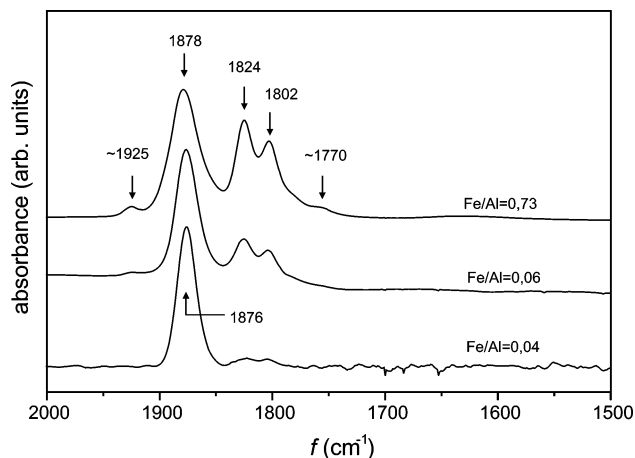


Figure 13. FTIR spectra of Fe-FER with Fe/Al of 0.04 (bottom), 0.08 (middle), and 0.73 (top) measured after adsorption of NO at 25 Torr.

in ferrierite at 1824 cm^{-1} and 1803 cm^{-1} corresponds to one broad intense band at 1813 cm^{-1} in Fe-ZSM-5. The low-intensity bands at ~ 1925 and ~ 1770 cm^{-1} correspond to bands at 1917 and 1769 cm^{-1} in Fe-ZSM-5. On the basis of the variation of band intensities with pressure, Berlier et al.²⁶ proposed an assignment to two adsorption clusters, dinitrosyl and trinitrosyl. Following their assignment for Fe-ZSM-5,²⁴ Fe-MCM-22,²⁵ and Fe-silicalite,²⁶ in ferrierite the triplet of modes at 1925, 1824, and 1803 cm^{-1} corresponds to a trinitrosyl species (Figure 13). The band at 1770 cm^{-1} corresponds to a low-frequency mode of a dinitrosyl species. The high-frequency component of the dinitrosyl species is not resolved (Figure 13). The similarity with the spectrum of ZSM-5 indicates that it should be located at ~ 1845 cm^{-1} between the intense band of mononitrosyl at 1876 cm^{-1} and the band of trinitrosyl at 1824 cm^{-1} .

NO stretching frequencies of $\text{Fe}-(\text{NO})_x$ adsorption clusters formed by a cation located in the β -1, β -2, α -1, or α -2 site, calculated by finite differences method corrected for anharmonicity, are collected in Table 4. The frequencies of a single adsorbed molecule ranging from 1877 to 1883 cm^{-1} compare well with the experimental band centered at 1876 cm^{-1} . The cluster in the α -1 site exhibits the frequency 1909 cm^{-1} representing the upper edge of the IR band. A large red-shift of the frequency by 83 and 190 cm^{-1} to 1798 and 1691 cm^{-1} is calculated for the *trans*-dinitrosyl clusters formed in the β -1 site. Similarly, large shifts by 68 and 167 cm^{-1} to 1815 and 1716 cm^{-1} are calculated for the *trans*-dinitrosyl cluster in the β -2 site. Such a pair of the low-frequency bands is, however, not observed in the IR spectrum (Figure 13), in agreement with the higher stability of *cis*- $\text{Fe}-(\text{NO})_2$ clusters.

Stable *cis*-dinitrosyl clusters are formed on the β -2, α -1, and α -2 sites (Figures 7–9). Stretching frequencies are calculated for both Fe-dinitrosyl and a Fe-dinitrosyl with additional NO

TABLE 4: Calculated NO Stretching Frequencies of Fe-(NO)_x, x = 1–3, Adsorption Clusters Formed in the β-1, β-2, α-1, and α-2 Sites of Fe-ferrierite^a

configuration/site	β-1	β-2	α-1	α-2
mononitrosyl	1881	1883	1909	1877
<i>trans</i> -dinitrosyl	1798, 1691	1815, 1716		
<i>cis</i> -dinitrosyl	1889, 1795	1887, 1824	1915, 1847	1868, 1820
<i>cis</i> -dinitrosyl + NO••Al		2019, 1827, 1769	2004, 1849, 1775	1988, 1857, 1782
<i>cis</i> -trinitrosyl		1869, 1849, 1839	1904, 1850, 1803	1903, 1847, 1779
<i>cis</i> -trinitrosyl + NO••Al		2034, 1925, 1840, 1807	2009, 1926, 1832, 1815	2000, 1928, 1847, 1814

^a Stretching frequencies in cm⁻¹ corrected for anharmonicity of 27 cm⁻¹.

molecule adsorbed on the Al site. Table 4 shows that adsorption of the additional NO molecule on the Al site considerably influences the stretching frequencies. The symmetric component of the stretching mode of the Fe-(NO)₂ complex is 1887, 1915, and 1868 cm⁻¹ for clusters in the β-2, α-1, and α-2 sites, respectively. After an additional NO molecule is adsorbed on the Al site, these frequencies decrease to 1827, 1849, and 1857 cm⁻¹. These values compare well with the symmetric component of a dinitrosyl²⁴ in Fe-ZSM-5 at 1845 cm⁻¹. Similarly, the frequency of the asymmetric component decreases from 1824, 1847, and 1820 cm⁻¹ to 1769, 1775, and 1782 cm⁻¹ for the β-2, α-1, and α-2 site, respectively, in good agreement with the weak intensity IR band at ~1770 cm⁻¹ observed for Fe-FER (Figure 13) or with the well-resolved band at 1769 cm⁻¹ in Fe-ZSM-5.²⁴ A combination of two stretching modes normally leads to symmetrical and asymmetrical components. The frequency of the former increases and of the latter decreases compared with the frequency of a single molecule. In the *cis*-dinitrosyls formed on the Fe²⁺ cation, both symmetric and asymmetric components of the stretching are downshifted. This probably happens because of the change of bonding induced by the adsorption of the second molecule (cf. text and Figure 12). The adsorption of an additional NO molecule on the Al site close to the *cis*-trinitrosyl complex leads to a change of the NO stretching frequencies as well. The frequency of one mode increases to 1925, 1926, and 1928 cm⁻¹ in the β-2, α-1, and α-2 site complex, respectively. This is comparable to the measured high-frequency band at ~1925 cm⁻¹ (Figure 13). The other two frequencies indicate the existence of two IR bands and agree reasonably well with the band maxima at 1824 and 1803 cm⁻¹ (Figure 13).

The stretching frequency of the additional molecule adsorbed on the Al site of *cis*-dinitrosyl is blue-shifted to 2019, 2004, and 1988 cm⁻¹ for the β-2, α-1, and α-2 site, respectively. The

corresponding frequencies of the *cis*-trinitrosyls with an additional NO adsorbed at the Al site are 2034, 2009, and 2000 cm⁻¹. As discussed above, the NO molecule adsorbed on the Al site of the di- and trinitrosyl is oxidized to form a NO⁺ cation. The interatomic distance is shortened to 1.123–1.129 Å, and the corresponding stretching frequency increases to 1988–2034 cm⁻¹ (Table 4). These frequencies correspond to the band appearing after oxidation of nitrosyl clusters formed on an Fe-exchanged zeolite²⁵ at 2000–2150 cm⁻¹.

Figure 14 shows IR spectra of adsorption clusters on the α-2 site derived from ab initio MD calculations. The vibrational spectra are calculated as Fourier transforms of the velocity autocorrelation functions. In the finite differences calculations of the vibrational eigenfrequencies, only forces induced by internal displacements within the Fe-(NO)_x or Fe-Al adsorption complexes are considered. The zeolite framework remains frozen. The ab initio MD simulations also account for the flexibility of the framework. However, these calculations are extremely time-consuming, and they are possible only by choosing values for the time step and duration of the simulation which represent a compromise between computational effort and accuracy. Because of the large time step of the molecular dynamics of Δt = 1 fs and too short simulation time of 2 ps, calculated stretching frequencies are uniformly shifted to lower frequencies. The comparison of the band maximum of the mononitrosyl at 1825 cm⁻¹ with experimental frequency of 1876 cm⁻¹ indicates a downshift of 51 cm⁻¹. In Figure 14, numbers in parentheses are band maxima shifted up by 51 cm⁻¹. The NO stretching frequencies of the dinitrosyl and trinitrosyl species derived from the MD simulation agree well with those calculated in the harmonic approximation and are corrected for anharmonicity as reported in Table 4. At the same time, the bands of the dinitrosyl and trinitrosyl species agree well with experimental IR bands reported above on ferrierite as well as with those reported on Fe-ZSM-5,²⁴ Fe-MCM-22,²⁵ and Fe-silicalite.²⁶ The NO⁺ stretching frequencies fall into the interval 2000–2150 cm⁻¹, where oxidation products appear in IR spectra of the Fe-exchanged zeolites.²⁵

5. Conclusions

An extensive study of NO adsorption over the Fe-exchanged ferrierite has been performed. The Fe²⁺ cation represents a strong adsorption center with adsorption energies of NO ranging from ~180 to ~240 kJ/mol. The cation exhibits a capacity to adsorb more than one NO molecule. In the most stable β-site, the Fe²⁺ cation can adsorb two and in all other locations three NO molecules. Bonding of a single NO molecule to Fe²⁺ is molecular and not dissociative upon NO adsorption. The nearly planar coordination of the cation by framework oxygens transforms to a square pyramid with the transition-metal cation slightly shifted away from the zeolite ring. The adsorption of two NO molecules changes the adsorption geometry of the cation except for the most stable configuration formed in the

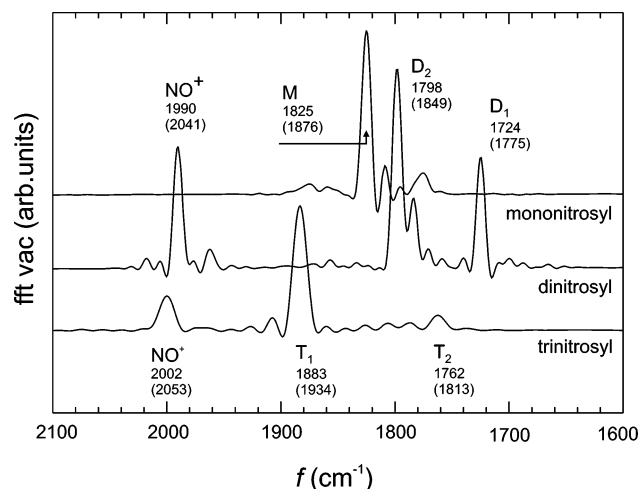


Figure 14. MD simulated IR spectra of adsorption clusters on α-2 site. M, D, and T stands for mono-, di-, and trinitrosyl species.

β -1 site. All other configurations are reconstructed to form a tetrahedral coordination of the transition-metal cation by the two NO molecules and only two framework oxygens, and the cation is shifted away from the zeolite ring. Multiple NO adsorption follows the same scenario for all configurations allowing a tetrahedral coordination. First, two NO molecules adsorb directly on the Fe^{2+} cation, a third molecule adsorbs to an Al site, and the fourth binds again to the cation. With four NO molecules, the Fe site is completely saturated. Tetrahedral coordination of the Fe^{2+} cation leads to two Fe–O bonds to the framework and two Fe–N bonds in a dinitrosyl species. In a trinitrosyl species, one Fe–O bond and three Fe–N bonds are formed. Upon adsorption of a single NO molecule on the Fe^{2+} cation, no activation of an Al site is observed. The formation of a tetrahedral coordination of the Fe^{2+} cation, however, leads to high adsorption power and strong oxidation properties of framework Al sites. The Al sites of three configurations exhibit adsorption energies as high as 92, 109, and 161 kJ/mol.

FTIR spectra of NO adsorbed on Fe-exchanged ferrierite show a multiplet of bands analogous to those observed on other Fe-exchanged zeolites (ZSM-5, MCM-22, silicalite). The calculated NO stretching frequencies agree with the experimentally observed peaks in the IR spectra and support the established assignment of spectral bands. Adsorption of a single NO molecule produces a single band centered at 1876 cm^{-1} . Two molecules adsorbed in a trans configuration and completing an octahedral coordination of the Fe^{2+} cation exhibit extremely downshifted frequencies. The asymmetric component of the stretching at approximately 1700 cm^{-1} is not observed in IR spectra. Well-distinguished, however, is the asymmetric component of the dinitrosyl species in a tetrahedral configuration at $\sim 1770\text{ cm}^{-1}$. Besides the band of a single NO molecule, the most intense bands are those originating from trinitrosyl species with a tetrahedral coordination of the Fe^{2+} cation at ~ 1925 , 1824 , and 1893 cm^{-1} . The adsorption at increased pressure of NO leads to the complete saturation of the coordination sphere of the Fe^{2+} cation. The $\text{Fe}(\text{NO})_3$ tetrahedron binds to one O atom of the framework and contains three adsorbed NO molecules. Interestingly, good agreement of calculated stretching frequencies is observed only for di- and trinitrosyl species with an additional NO molecule adsorbed on the Al site. This indicates that at increased NO pressure both the Fe^{2+} cations and Al sites are saturated. The adsorption power of the Al site develops when two molecules adsorb on the Fe^{2+} cation producing an $[\text{Fe}-(\text{NO})_2]^+$ complex. The decrease of the charge of the extraframework particle leads to concerted oxidation of the third NO molecule adsorbed on the Al site producing a NO^+ cation long-lived on the inner surface of the zeolite.

Acknowledgment. This work has been supported by the Austrian Science Fund under project No. P17020-PHYS and by the Institut Français du Pétrole. Computational resources are partly granted by the Computing Center of Vienna University (Schrödinger II). The work in Prag was supported by the Grant Agency of the Academy of Sciences of the Czech Republic under Project IET 400400413.

References and Notes

- (1) Li, Y.; Armor, J. N. *Appl. Catal., B: Environ.* **1992**, *1*, L21.
- (2) Kapteijn, F.; Rodrigues-Mirasol, J.; Moulijn, J. A. *Appl. Catal., B: Environ.* **1996**, *9*, 25.
- (3) Turek, T. J. *Catal.* **1998**, *174*, 98.
- (4) Kapteijn, F.; Marban, G.; Rodrigues-Mirasol, J.; Moulijn, J. A. *J. Catal.* **1997**, *167*, 256.
- (5) Perez-Ramirez, J.; Kapteijn, F.; Mul, G.; Moulijn, J. A. *J. Catal.* **2002**, *208*, 211.
- (6) Wood, B. R.; Reimer, J. A.; Bell, A. T. *J. Catal.* **2002**, *209*, 151.
- (7) Zhu, Q.; van Teeffelen, R. M.; van Santen, R. A.; Hensen, E. M. *J. Catal.* **2004**, *221*, 573.
- (8) Perez-Ramirez, J.; Kapteijn, F.; Schoffel, K.; Moulijn, J. A. *Appl. Catal., B: Environ.* **2003**, *44*, 117.
- (9) Mul, G.; Perez-Ramirez, J.; Kapteijn, F.; Moulijn, J. A. *Catal. Lett.* **2001**, *77*, 7.
- (10) Perez-Ramirez, J.; Mul, G.; Kapteijn, F.; Moulijn, J. A. *Kinet. Catal.* **2003**, *44*, 639.
- (11) Perez-Ramirez, J.; Kumar, M. S.; Bruckner, A. J. *J. Catal.* **2004**, *223*, 13.
- (12) Dubkov, K. A.; Ovanesyan, N. S.; Shteinman, A. A.; Starokon, E. V.; Panov, G. I. *J. Catal.* **2002**, *207*, 341.
- (13) Sang, C.; Kim, B. H.; Lund, C. R. F. *J. Phys. Chem. B* **2005**, *109*, 2295.
- (14) Yakovlev, A. L.; Zhidomirov, G. M.; van Santen, R. A. *Catal. Lett.* **2001**, *75*, 45.
- (15) Kachurovskaya, N. A.; Zhidomirov, G. M.; Hensen, E. J. M.; van Santen, R. A. *Catal. Lett.* **2003**, *86*, 25.
- (16) Yakovlev, A. L.; Zhidomirov, G. M.; van Santen, R. A. *J. Phys. Chem. B* **2001**, *105*, 12297.
- (17) Yoshizawa, K.; Yumura, T.; Shirota, Y.; Yamabe, T. *Bull. Chem. Soc. Jpn.* **2000**, *73*, 29.
- (18) Yoshizawa, K.; Shirota, Y.; Yumura, T.; Yamabe, T. *J. Phys. Chem. B* **2000**, *104*, 734.
- (19) Ryder, J. A.; Chakraborty, A. K.; Bell, A. T. *J. Phys. Chem. B* **2002**, *106*, 7059.
- (20) Heyden, A.; Peters, B.; Bell, A. T.; Keil, F. J. *J. Phys. Chem. B* **2005**, *109*, 1857.
- (21) Heyden, A.; Hansen, N.; Bell, T. A.; Keil, F. J. *J. Phys. Chem. B* **2006**, *110*, 17096.
- (22) Kachurovskaya, N. A.; Zhidomirov, G. M.; van Santen, R. A. *J. Phys. Chem. B* **2004**, *108*, 5944.
- (23) Benco, L.; Bucko, T.; Grybos, R.; Hafner, J.; Sobalik, Z.; Dedecek, J.; Hrusak, J. *J. Phys. Chem. C* **2007**, *111*, 586.
- (24) Berlier, G.; Zecchina, A.; Spoto, G.; Ricchiardi, G.; Bordiga, S.; Lamberti, C. *J. Catal.* **2003**, *215*, 264.
- (25) Berlier, G.; Pourny, M.; Bordiga, S.; Spoto, G.; Zecchina, A.; Lamberti, C. *J. Catal.* **2005**, *229*, 45.
- (26) Berlier, G.; Spoto, G.; Bordiga, S.; Ricchiardi, G.; Fiscaro, P.; Zecchina, A.; Rosetti, I.; Selli, E.; Forni, L.; Giamello, E.; Lamberti, C. *J. Catal.* **2002**, *208*, 64.
- (27) Mortier, W. J. *Compilation of Extra-framework Sites in Zeolites*; Butterworths: London, 1982.
- (28) Pickering, I. J.; Maddox, P. J.; Thomas, J. M.; Cheetham, A. K. *J. Catal.* **1989**, *119*, 261.
- (29) Wichterlova, B.; Sobalik, Z.; Dedecek, J. *Appl. Catal., B: Environ.* **2003**, *41*, 97.
- (30) Kresse, G.; Hafner, J. *Phys. Rev. B* **1993**, *48*, 13115.
- (31) Kresse, G.; Hafner, J. *Phys. Rev. B* **1994**, *49*, 14251.
- (32) Kresse, G.; Furthmuller, J. *Comput. Mater. Sci.* **1996**, *6*, 15.
- (33) Kresse, G.; Furthmuller, J. *Phys. Rev. B* **1996**, *54*, 11169.
- (34) Nose, S. *J. Chem. Phys.* **1984**, *81*, 511.
- (35) Allen, M. P.; Tildesley, D. J. *Computer Simulations of Liquids*; Clarendon: Oxford, U.K., 1987.
- (36) Kresse, G.; Furthmuller, J.; Hafner, J. *Europhys. Lett.* **1995**, *32*, 729.
- (37) Ugliengo, P. Program ANHARM. University of Torino, 1989.
- (38) Dedecek, J.; Gabova, V.; Wichterlova, B. *Stud. Surf. Sci. Catal.* **2002**, *142*, 1817.